Role of the lateral channel in catalase HPII of Escherichia coli

MS Sevinc, MJ Mate, J Switala, I Fita and PC Loewen

Protein Sci. 1999 8: 490-498
Access the most recent version at doi:10.1110/ps.8.3.490

Protein Science (1999), *8*:490–498. Cambridge University Press. Printed in the USA.

Role of the lateral channel in catalase HPII of *Escherichia coli*

M. SERDAL SEVINC,[1] MARIA J. MATÉ,[2] JACK SWITALA,[1] IGNACIO FITA,[2] AND PETER C. LOEWEN[1]

[1]Department of Microbiology, University of Manitoba, Winnipeg, Manitoba R3T 2N2, Canada
[2]Departamento de Biología Molecular y Celular, CID (CSIC), Jordi Girona 18–26, 08034 Barcelona, Spain

(RECEIVED July 20, 1998; ACCEPTED November 19, 1998)

Abstract

The heme-containing catalase HPII of *Escherichia coli* consists of a homotetramer in which each subunit contains a core region with the highly conserved catalase tertiary structure, to which are appended N- and C-terminal extensions making it the largest known catalase. HPII does not bind NADPH, a cofactor often found in catalases. In HPII, residues 585–590 of the C-terminal extension protrude into the pocket corresponding to the NADPH binding site in the bovine liver catalase. Despite this difference, residues that define the NADPH pocket in the bovine enzyme appear to be well preserved in HPII. Only two residues that interact ionically with NADPH in the bovine enzyme (Asp212 and His304) differ in HPII (Glu270 and Glu362), but their mutation to the bovine sequence did not promote nucleotide binding. The active-site heme groups are deeply buried inside the molecular structure requiring the movement of substrate and products through long channels. One potential channel is about 30 Å in length, approaches the heme active site laterally, and is structurally related to the branched channel associated with the NADPH binding pocket in catalases that bind the dinucleotide. In HPII, the upper branch of this channel is interrupted by the presence of Arg260 ionically bound to Glu270. When Arg260 is replaced by alanine, there is a threefold increase in the catalytic activity of the enzyme. Inhibitors of HPII, including azide, cyanide, various sulfhydryl reagents, and alkylhydroxylamine derivatives, are effective at lower concentration on the Ala260 mutant enzyme compared to the wild-type enzyme. The crystal structure of the Ala260 mutant variant of HPII, determined at 2.3 Å resolution, revealed a number of local structural changes resulting in the opening of a second branch in the lateral channel, which appears to be used by inhibitors for access to the active site, either as an inlet channel for substrate or an exhaust channel for reaction products.

Keywords: catalase; crystal structure; inhibitor access; substrate channels

Catalase (hydrogen peroxide:hydrogen peroxide oxidoreductase, EC 1.11.1.6), present in most aerobic organisms, is a protective enzyme that removes hydrogen peroxide before it can decompose into highly reactive hydroxyl radicals. The reaction of catalase utilizes hydrogen peroxide as both an electron donor and acceptor in the following reaction: $2H_2O_2 \rightarrow 2H_2O + O_2$.

The structures of six catalases have now been solved including those from bovine liver (BLC) (Murthy et al., 1981; Fita et al., 1986), *Penicillium vitale* (PVC) (Vainshtein et al., 1981, 1986), *Proteus mirabilis* (PMC) (Gouet et al., 1995), *Micrococcus lysodeikticus* (MLC) (Murshudov et al., 1992), *Saccharomyces cerevisiae* (SCCA) (Berthet et al., 1997; Maté et al., 1999), and *Escherichia coli* (HPII) (Bravo et al., 1995; Bravo et al., 1998) revealing a common highly conserved core in all enzymes. From these structures, significant insights into the enzymatic mechanisms and novel structural features have been gained.

Some catalases, including the small subunit enzymes from bovine liver, yeast, *P. mirabilis* and *M. lysodeikticus*, have NADPH bound, but others, including the large subunit enzymes from *P. vitale* and *E. coli* (Hillar et al., 1994), do not. It has been hypothesized that the role of the nucleotide is to prevent the accumulation of inactive compound II by promoting its reduction to ground state Fe^{+++} (Hillar & Nicholls, 1992). According to this hypothesis, the large subunit catalase HPII, which does not form compound II, does not need to bind NADPH (Hillar & Nicholls, 1992).

The refined HPII structure at 1.9 Å has revealed a complex network of channels reaching close to the heme pocket (Bravo et al., 1998). One channel, over 50 Å in length, begins in the interface between the C-terminal domain and the core of an adjacent subunit and eventually bends so that it approaches the heme distal side pocket perpendicular to the plane of the heme. This is an elongated equivalent of the main channel identified in BLC (Fita et al., 1986). A second channel approaches the heme active site

Reprint requests to: Peter C. Loewen, Department of Microbiology, University of Manitoba, Winnipeg, Manitoba R3T 2N2, Canada; e-mail: Peter_Loewen@umanitoba.ca.

laterally, beginning on the surface of the HPII subunit at a location corresponding to the NADPH pocket in catalases that bind the dinucleotide. This second channel is structurally related to the bifurcated channel associated with the NADPH binding pocket in catalases that bind the nucleotide (Gouet et al., 1995; Maté et al., 1999). The role of this lateral channel was postulated to involve NADPH in BLC, but it must have a different role in HPII, which lacks the dinucleotide. The presence of multiple channels suggested the possibility of separate inlet and outlet functions for each channel, such that the reaction products could be exhausted from the active site without interfering with the incoming substrate. This may be one of the mechanisms by which the enzyme maintains a high turnover rate despite a deeply buried and inaccessible active site. Still another channel leading to the proximal side of the heme can be postulated in HPII, which might be the access path for the substrate required for heme *b* to heme *d* conversion (Murshudov et al., 1996) and formation of the His-Tyr bond (Bravo et al., 1997). All these molecular channels contain solvent molecules that are clearly defined in the electron density maps of the refined structure of native HPII.

This paper reports an investigation of the region of HPII that corresponds to the NADPH binding region of BLC and the lateral channel. A number of mutations were introduced into this region and the properties of these mutant variants, including their specific activities and sensitivities to various inhibitors, are interpreted in terms of a role for the lateral channel in HPII.

Results

Comparison of the NADPH binding region of BLC with the homologous region of HPII

The stereo diagram in Figure 1 shows the structure of the region of HPII, which is analogous to the NADPH binding site of BLC. The NADPH molecule, as found in BLC, is superimposed on the HPII structure to assess the differential interactions to explain why it does not bind to HPII. Also, two structural reasons for the lack of NADPH in HPII can be proposed. Residues 585–590, a segment of the HPII C-terminal extension which does not exist in BLC, protrude into the NADPH pocket of BLC and interfere with the possible binding of NADPH. A second reason can be the change in HPII of two of four residues that make ionic interactions with NADPH in BLC. Residues Asp212 and His304 of BLC have been changed at the equivalent sites in HPII to Glu270 and Glu362. Two other residues predicted to interact with NADPH in BLC, Arg202 and Lys236, are conserved as Arg260 and Lys294 in HPII. In the absence of NADPH in HPII, the residues that might have been involved in dinucleotide binding should have alternative interactions. This is the case, for example, with Arg260 being associated in an ionic interaction with Glu270, equivalent to Asp212 in BLC.

Mutation of residues in the putative NADPH binding cavity

Two mutations, Glu270Asp and Glu362His, were introduced into *katE*, individually and together, to generate a BLC counterpart of HPII with respect to residues interacting through salt bridges with NADPH. All three mutant enzymes exhibited problems in folding such that more enzyme was produced at 28 °C than at 37 °C (Table 1). This has been observed for other mutant variants of HPII, and explained in terms of a lower proteolysis rate at 28 °C, that allows chaperones more time to promote proper folding (Sevinc et al., 1998). Following purification from cells grown at 28 °C, the mutant enzymes were found to have equivalent or slightly higher activity than the wild-type enzyme (Table 1). The UV-visible absorption spectra and the heme composition of the mutant enzymes were indistinguishable from similar data for the wild-type enzyme (data not shown). A simple fluorescence assay for NADPH revealed no increase in fluorescence over that of the wild-type enzyme that would be indicative of no NADPH being bound (data not shown). This confirmed that the residue changes were not the sole factors in preventing NADPH binding to HPII and that the

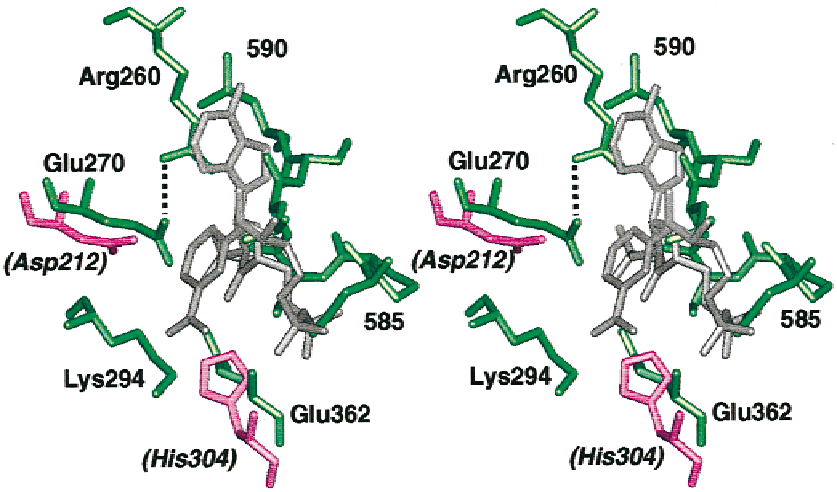

Fig. 1. Stereo diagram of the region of HPII that corresponds to the NADPH binding pocket of BLC. The residues Arg260, Glu270, Lys294, and Glu362 (all green) are shown. The segment extending between residues 585 and 590 is shown also colored in green. The NADPH from BLC (colored gray) is superimposed on the HPII structure, as are the BLC residues Asp212 and His304 (both purple) that correspond to Glu270 and Glu362 of HPII. The steric overlap of the NADPH of BLC, and segments of the 585–590 sequence of HPII is evident.

Table 1. *Catalase activity in crude extracts of cultures producing mutant variants of HPII, and specific activity of purified catalase protein*

Mutant	Crude extract activity (units/mg dry cell weight) 28 °C[a]	37 °C[a]	Purified enzyme activity (units/mg)
Wild-type	388 ± 59	425 ± 51	14,322
E270D	268 ± 47	71 ± 6	16,137
E362H	305 ± 61	145 ± 9	18,325
E270D/E362H	115 ± 23	10 ± 1	16,589
R260A	273 ± 28	88 ± 16	35,891
K294A	297 ± 43	91 ± 16	18,635
R260A/K294A	27 ± 7	2 ± 0.5	12,880

[a]Denotes the temperatures at which the cultures were grown for 16 h prior to catalase assay.

presence of the segment containing residues 585–590 is, most probably, the dominant factor.

The role of the Arg260 and Lys294 side chains in the absence of NADPH was addressed by changing the two residues to alanine, individually and together. The singly mutated enzymes, containing Arg260Ala and Lys294Ala changes, exhibited minor folding problems with threefold higher levels of enzyme activity being evident in cells grown at 28 °C as compared to 37 °C. The double mutant variant, Arg260Ala/Lys294Ala, exhibited an even greater folding defect and accumulated less than 10% of wild-type levels even at 28 °C. Despite the folding problems, equivalent (the Ala294 and Ala260/Ala294 variants), or threefold higher (the Ala260 variant), specific activities were observed for the purified enzymes as compared to the wild-type HPII (Table 1). There were no differences from the wild-type enzyme in either the UV-visible spectra or in heme content of any of the mutants (data not shown). The influence of H_2O_2 concentration on turnover rate of the wild-type and Ala260 mutant variant was determined revealing similar kinetic responses, but a threefold higher k_{cat} for the mutant enzyme (Fig. 2). The response of BLC to $[H_2O_2]$ reveals a much higher turnover rate at low $[H_2O_2]$, but much greater sensitivity to higher $[H_2O_2]$ as compared to HPII. The o-dianisidine peroxidatic activity of wild-type HPII is very low at less than 0.001 units/mg, and this was not increased by the Arg260Ala mutation.

Effect of inhibitors on the Ala260 mutant variant of HPII

The threefold higher catalytic specific activity and turnover rate of the Ala260 mutant variant of HPII was surprising because of the remoteness of the mutation from the active site. One possible explanation for the enhanced activity of the Ala260 mutant variant relative to the wild-type HPII was easier access of the substrate to the active site. Because both the perpendicular and lateral channels leading to the active site have regions where the dimensions are at the limit of what will allow access of the substrate H_2O_2, small changes in dimensions might have significant effects on substrate access. This was investigated by comparing the effect on the two enzymes of various inhibitors, starting with azide and cyanide. The Ala260 mutant protein was slightly more sensitive to cyanide than wild-type (Fig. 3A), and it was significantly more sensitive to

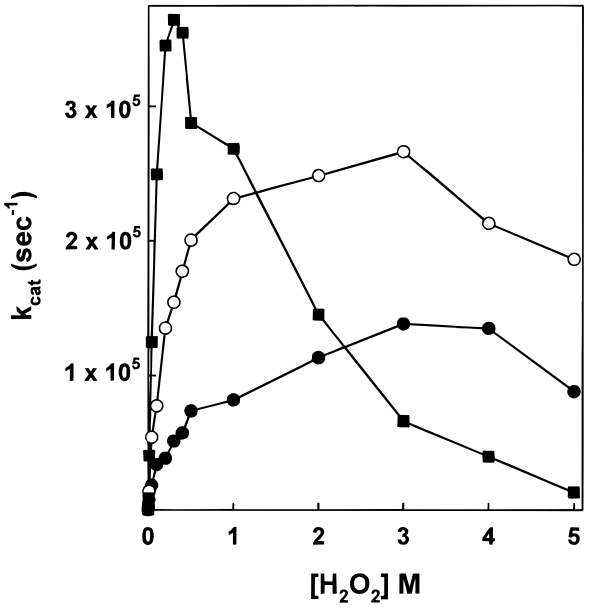

Fig. 2. Effect of hydrogen peroxide concentration on the turnover rate or catalytic efficiency of wild-type HPII (●), the Ala260 mutant variant of HPII (○), and BLC (■). Initial rates of oxygen evolution were used to determine the enzyme activity.

azide (Fig. 3B). The 50% inhibitory concentration of cyanide on the wild-type enzyme was slightly higher as compared to the Ala260 mutant variant (15 and 12 mM, respectively), whereas the 50% inhibitory concentration for azide was significantly higher for the wild-type compared to the mutant variant (260 and 45 mM, respectively). Therefore, differences in access to the active site between the two enzymes have a greater effect on azide than on the smaller cyanide.

The inhibitory properties of a number of hydroxylamine derivatives were also investigated including hydroxylamine, O-methyl

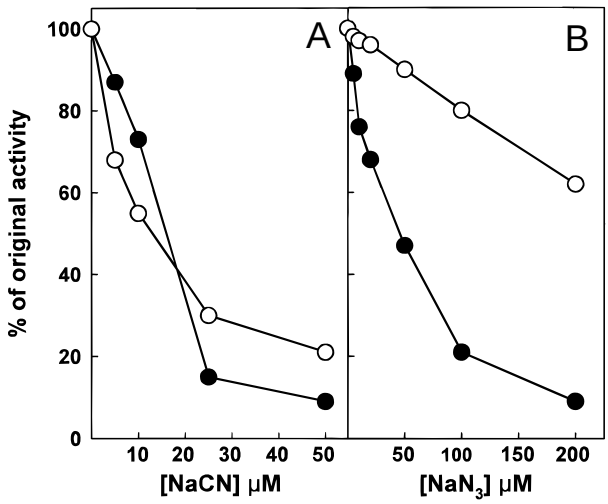

Fig. 3. Inhibition of wild-type HPII (○) and the Ala260 variant (●) by (**A**) NaCN and (**B**) NaN_3. The enzyme was incubated with the various concentrations of the inhibitors for 1 min at 37 °C before beginning the assay by adding H_2O_2.

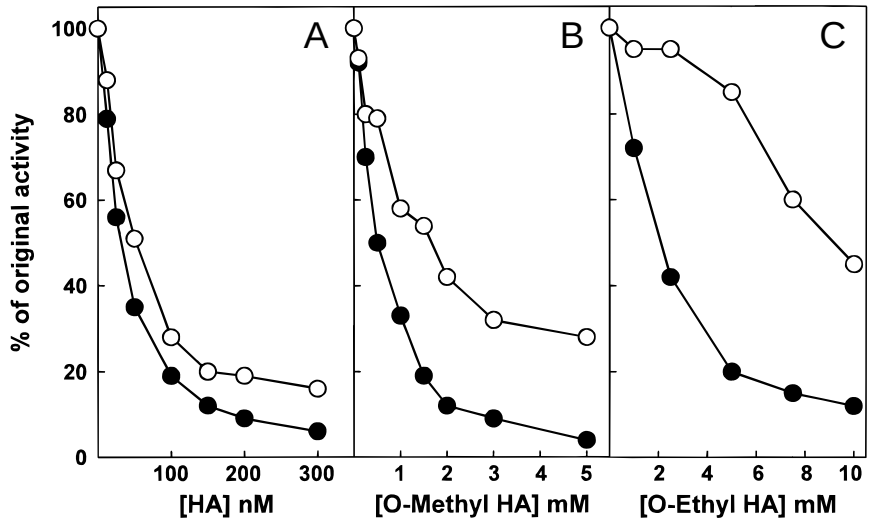

Fig. 4. Inhibition of wild-type HPII (○) and the Ala260 variant (●) by (**A**) hydroxylamine or HA, (**B**) O-methylhydroxylamine or O-Methyl HA, and (**C**) O-ethylhydroxylamine or O-EthylHA. The enzyme was incubated with various concentrations of the inhibitor for 1 min at 37 °C before beginning the assay by adding H_2O_2.

hydroxylamine, and O-ethyl hydroxylamine. In all cases, the mutant variant was more sensitive than the wild-type enzyme (Fig. 4), particularly for the larger alkylhydroxylamine derivatives (Fig. 4B,C). The 50% inhibitory concentrations reveal less than a twofold difference for hydroxylamine on the two enzymes (50 and 30 nM, respectively, for the wild-type and Ala260 variants); and a greater than threefold difference for O-methyl hydroxylamine (1.6 and 0.5 mM, respectively, for the wild-type and Ala260 variants) and O-ethyl hydroxylamine (8.7 and 1.8 mM, respectively, for the wild-type and Ala260 variants). In addition to demonstrating the difference between enzyme variants, the 100-fold lower effective concentration of hydroxylamine as compared to its larger alkyl derivatives demonstrates the selectivity of the access channels.

To investigate further the size limits on accessibility, sulfhydryl reagents, known inhibitors of catalase, which come in a range of sizes (Takeda et al., 1980; Shimizu et al., 1984; Sevinc et al., 1998), were studied including 2-mercaptoethanol, dithiothreitol, cysteine, and glutathione. The smallest of this group, 2-mercaptoethanol, had a similar inhibitory effect on both the Ala260 mutant and HPII (Fig. 5A). The larger reagents all showed differential effects on the two enzymes roughly consistent with their size differences. Dithiothreitol showed the most striking difference (Fig. 5B) while the largest molecule, glutathione, was not able to access the HPII active site but caused partial inhibition of the Ala260 mutant enzyme (Fig. 5D).

Changes in the absorption spectra of the enzymes caused by the sulfhydryl agents were also consistent with a change in the accessibility of the active sites. The two smallest reagents, mercaptoethanol and dithiothreitol, caused a larger increase in absorbance at 630 nm (Fig. 6) for the Ala260 mutant variant compared to the wild-type enzyme. The two largest reagents, Cys and GSH, were apparently unable to access the heme sufficiently to cause any spectral changes.

Structural changes in the Ala260 variant of HPII

The crystal structure of the Ala260 mutant variant of HPII, determined and refined to 2.3 Å resolution, gives crystallographic agreement factors R and R_{free} of 20.0% and 26.7%, respectively. All the significant peaks in difference Fourier maps between native and mutant structures are situated in the vicinity of the mutated residue (Fig. 7A). These maps clearly show: (1) the expected absence of

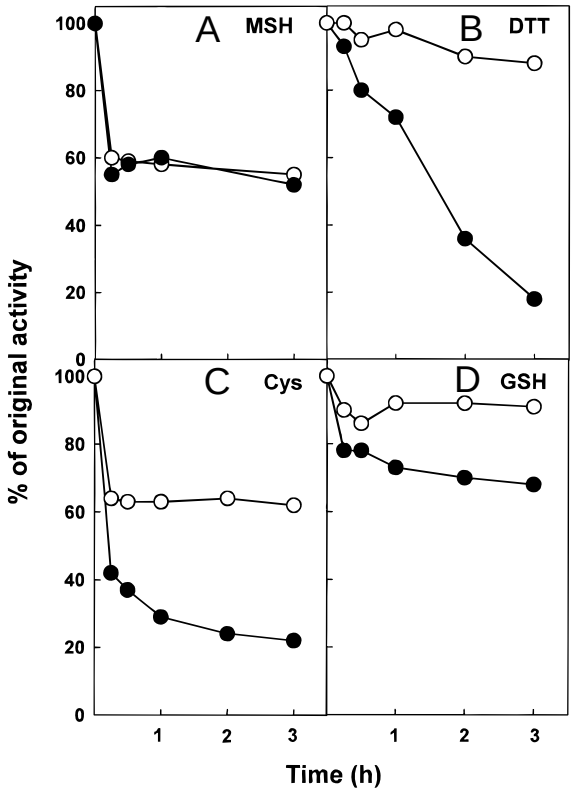

Fig. 5. Inhibition of wild-type HPII (○) and the Ala260 variant (●) by 5 mM each of 2-mercaptoethanol (A MSH), dithiothreitol (B DTT), cysteine (C Cys), and glutathione (D GSH). The enzyme and sulfhydryl reagent were incubated at 37 °C and aliquots were removed at various times for catalase assay.

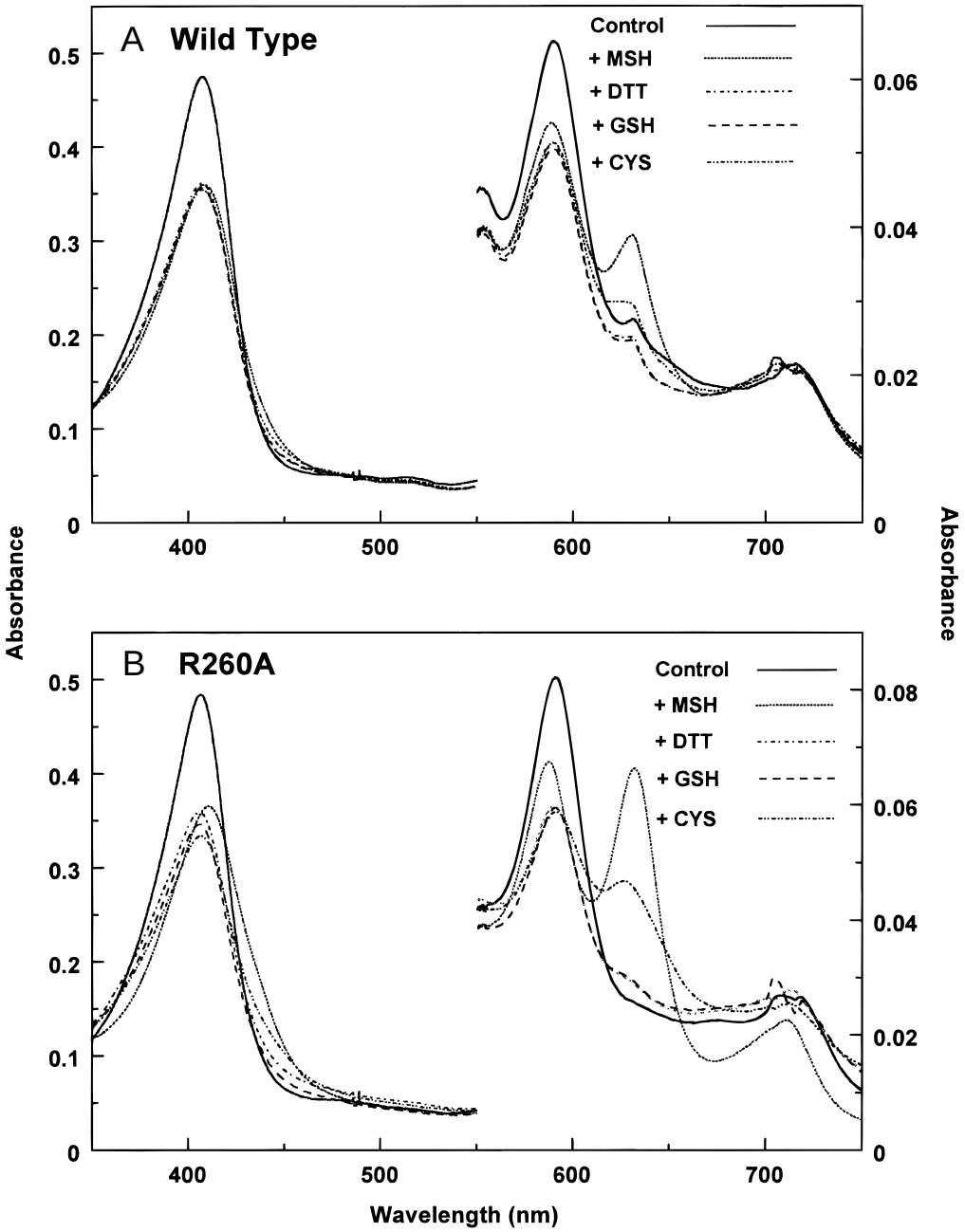

Fig. 6. Effect of various sulfhydryl agents on the UV-visible absorption spectra of wild-type HPII and the Ala260 variant. Spectra were measured after the enzyme had been incubated with the enzyme for 3 h at 20 °C. The left axis corresponds to the range from 350–550 nm and the right axis corresponds for the range from 550–750 nm.

the Arg260 side chain; (2) changes in the nearby solvent structure including the presence of new water molecules; (3) the high mobility of the Glu270 side chain that is poorly defined in the mutant structure, but is clearly defined in a salt bridge with Arg260 in the wild-type enzyme; and (4) other residues in this region that exhibit significant increases in their temperature factors in the mutant relative to those in the wild-type enzyme. The cumulative effect of these changes is an increase in the static solvent accessibility in the vicinity of residue 260 in the mutant structure (Fig. 7B). If the variable positions of the side-chain atoms from Glu270 are omitted during the accessibility calculations, a continuous channel reaching close to the heme distal pocket, above Asn201, can be defined (Fig. 7B). This new opening is structurally related to the upper branch of the lateral channel recently described for catalases that bind NADPH (Maté et al., 1999). The flow of substances along this new opening might also be facilitated by the increased mobility of most residues in its vicinity.

Discussion

Replacement of the arginine side chain with the methyl group of alanine in the Ala260 mutant variant of HPII results in only minor

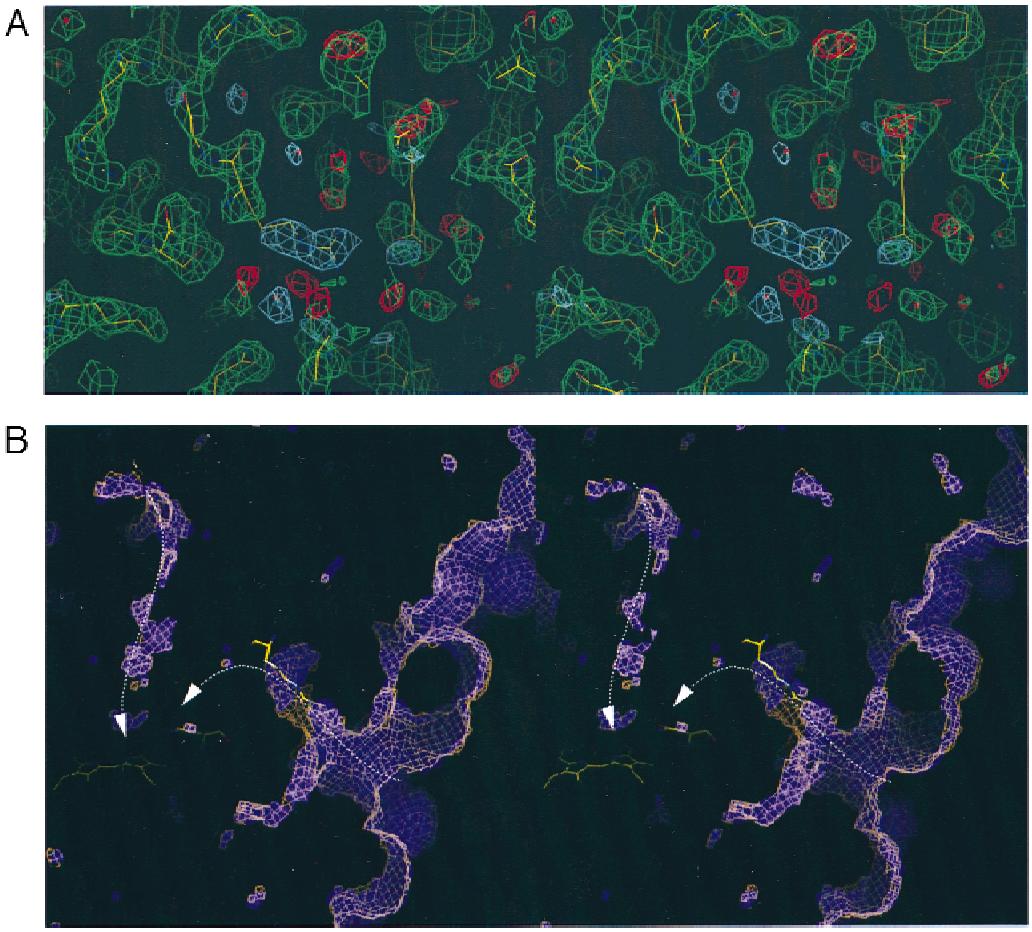

Fig. 7. A: Stereo view of the electron density maps for the Ala260 mutant variant of HPII (F_c calculated from the native model). The $2F_o - F_c$ map is represented in green, and the $F_o - F_c$ map at 3.0 and −3.0 sigma level are represented in red and gray, respectively. The absence of the Arg260 side chain (gray), and of some water molecules (also gray) together with the presence of a few new solvent molecules (red), makes the disorder in the side chain of Glu270 apparent. **B:** Accessibility surface calculated using the program VOIDOO. The heme group and residues Asn201 and Arg260, as determined in the native structure, are explicitly shown with balls and sticks. The blue surface corresponds to the solvent accessibility for the Ala260 mutant variant of HPII. When side-chain atoms from Glu270 are also omitted, the resulting accessible surface is indicated as a yellow grid in this figure. A single arrow indicates the entry channel and a double arrow is used to indicate the lateral channel the may be both an entry and exit channel.

structural changes. Moreover, all of these changes are localized in the vicinity of the mutated residue more than 15 Å from the heme iron atom. Despite the lack of direct influence on the active site, the mutant enzyme shows a threefold increase in the catalytic activity and a threefold to fivefold greater sensitivity toward bulky inhibitors. The analysis of changes in solvent accessibility provides a possible explanation for this apparent paradox. The removal of the large Arg260 side chain and consequent disruption of the Arg260–Glu270 salt bridge creates an enlarged new opening that could act as a supplementary route to reach the active center in the mutant enzyme.

The Ala260 mutant variant of HPII does not show a significant increment in its sensitivity toward cyanide, which has approximately the same size as the substrate hydrogen peroxide, which also seems to have easier access in the mutant. This may be the result of the reactions of cyanide and other inhibitors not being limited by their access to the heme, because once they are bound they have only a slow exchange rate. On the other hand, the catalytic reaction is a progressive reaction involving the continual ingress of substrate peroxide and the continual egress of reaction products oxygen and water. The increase in the catalytic turnover rate of the mutant variant could arise from easier inlet of substrate or easier exhaust of product. The lack of any substantial effect of the Arg260Ala mutation on the peroxidatic activity utilizing the large organic substrate o-dianisidine would seem to be inconsistent with the enlarged channel acting as an inlet or exhaust path. However, this observation can also indicate that the peroxidatic activity of HPII is low not because of restricted access, but mainly because it is an unfavorable reaction in the large catalases. Despite these ambiguities, in particular with respect to the mechanism used by the mutant to increase the catalytic activity, the present results provide clear evidence that the lateral channel can be used in catalases to access the active site. In NADPH containing catalases, the upper branch on the lateral channel, structurally equivalent to the new opening in the Ala260 mutant variant of HPII, appears to be sterically restricted at its entrance by the presence of the dinucleotide.

Evidence supporting a role for the channel perpendicular to the heme is limited to the report of mutant variants of SSCA in which residues at the entrance to the distal side pocket were changed to

smaller residues (Zamocky et al., 1995; Maté et al., 1999). These changes resulted in enhanced peroxidatic activity, which suggested that access to the active site for larger substrates had been improved, but in reduced catalytic activity. This indicated that faster diffusion could not compensate for the loss of optimal interactions that may pre-orient the hydrogen peroxide in the active-site pocket. In the case of the mutant variant of HPII, the location of the mutation does not affect the active-site pocket and faster diffusion of substrates or products might be the explanation for the increased catalytic activity. The catalytic activities of HPII and the mutant variant are, in any case, lower than the activities of the smaller subunit catalase, BLC, which could be related to the peculiarities and 20 Å greater length of the channel perpendicular to the heme in HPII.

In spite of the differences between large and small subunit catalases and the ambiguities remaining in a clear definition of the inlet and exhaust channels, a unified view of the role of the molecular channels might be summarized as follows. The channel perpendicular to the heme can be considered the main entrance for the peroxide substrate because: (1) the increased peroxidatic activity in SCCA when the channel is enlarged; (2) the organization of this channel appears to be optimized for bringing hydrogen peroxide into the active-site heme pocket; and (3) the lateral channel in small subunit catalases contains NADPH as an obstacle. Because of its small diameter, the perpendicular channel cannot act simultaneously as an exit path for reaction products during the fast catalytic turnover, and the lateral channel provides the required exit path. Accessibility to the heme active site through the lateral channel in wild-type HPII appears to be restricted, possibly to regulate the flow of substances along it. Enlarging the channel, as with the Arg260Ala mutation, not only allows easier exhaust of reaction products but opens the channel for the larger inhibitors to access the active site.

Materials and methods

Materials

Standard chemicals and biochemicals were obtained from Sigma Chemical Co. (St. Louis, Missouri). Restriction nucleases, polynucleotide kinase, DNA ligase, and the Klenow fragment of DNA polymerase were obtained from GIBCO-BRL.

Strains and plasmids

The plasmid pAMkatE72 (von Ossowski et al., 1991) was used as the source for the *katE* gene. Phagemids pKS+ and pKS− from Stratagene Cloning Systems were used for mutagenesis, sequencing, and cloning. *E. coli* strains NM522 (*supE thi*) (*lac-proAB*) *hsd-5* [F′ *proAB lacI*^{q} *lacZ*Δ*15*]) (Mead et al., 1985), JM109 (*recA1 supE44 endA1 hsdR17 gyrA96 relA1 thi* Δ(*lac-proAB*) (Yanisch-Perron et al., 1985), and CJ236 (*dut-1 ung-1 thi-1 relA1*/pCJ105 F′) (Kunkel et al., 1987) were used as hosts for the plasmids and for generation of single-strand phage DNA, using helper phage R408. Strain UM255 (*pro leu rpsL hsdM hsdR endI lacY katG2 katE12::*Tn*10 recA*) (Mulvey et al., 1988) was used for expression of the mutant *katE* constructs and isolation of the mutant HPII proteins.

Oligonucleotide-directed mutagenesis

Oligonucleotides were synthesized on a PCR-Mate synthesizer from Applied Biosystems and are listed in Table 2. The restriction nuclease fragments that were mutagenized following the Kunkel procedure (Kunkel et al., 1987), sequenced and subsequently reincorporated into pAMkatE72 to generate the mutagenized *katE* genes, are also listed. Sequence confirmation of all sequences was by the Sanger method (Sanger et al., 1977) on double-stranded plasmid DNA generated in JM109. Subsequent expression and purification were carried out as previously described (Loewen et al., 1993).

Catalase, protein, and spectral determination

Catalase activity was determined by the method of Rørth and Jensen (1967) in a Gilson oxygraph equipped with a Clark electrode. One unit of catalase is defined as the amount that decomposes 1 μmol of H_2O_2 in 1 min in a 60 mM H_2O_2 solution at pH 7.0 at 37 °C. Initial rates of oxygen evolution were used to determine the turnover rates to minimize the inactivation caused by high $[H_2O_2]$ (Ogura, 1955). Protein was estimated according to the methods outlined by Layne (1957). Absorption spectra were obtained using a Milton Roy MR3000 spectrophotometer. Samples were dissolved in 50 mM potassium phosphate, pH 7.0.

Enzyme purification

Cultures of *E. coli* strain transformed with plasmids pAMkatE72 (von Ossowski et al., 1991), pR260A, pK294A, and pR260A/K294A, encoding HPII or the Ala260, Ala294 and Ala260/Ala294 mutant varitants, respectively, were grown in Luria broth containing 10 g/L tryptone, 5 g/L yeast extract, and 5 g/L NaCl. Growth of the mutant variants was for 22 h at 28 °C and of the wild-type HPII for 16 h at 37 °C with shaking. Cells were harvested and HPII

Table 2. *Oligonucleotides and katE restriction fragments used in oligonucleotide-directed mutagenesis of katE*

Mutant	Sequence change	Oligonucleotide[a]	Restriction fragment
E270D	(GAA→GAT)	CGCACCATC**GAT**GGCTTCGGT	*Hin*dIII-EcoRI (1246–1856)
E362H	(GAA→CAC)	CTTATCCCG**CAC**GAACTGGTG	*Eco*RI-*Cla*I (1856–3466)
R260A	(CGC→GCC)	GATGTCGGAT**GCC**GGCATCCCC	*Hin*dIII-EcoRI (1246–1856)
K294A	(AAA→GCA)	TTTCCACTGG**GCA**CCACTGGCA	*Hin*dIII-EcoRI (1246–1856)

[a]The sequence in bold is the codon that has been modified.

was isolated as previously described (Loewen & Switala, 1986). Following resuspension of the ammonium sulfate fraction, the solution was heated at 50° C for 15 min followed by centrifugation prior to chromatography on DEAE cellulose (Whatman).

Crystallization, data collection, and refinement

Crystals of the Ala260 variant of HPII were obtained at 22 °C using the hanging drop vapor diffusion method over a reservoir solution containing 15–17% PEG 3350 (Carbowax), 1.6–1.7 M LiCl (Baker), and 0.1 M Tris pH 9.0. High resolution data were collected using a rotating anode X-ray source, a graphite monochrometer, and an imaging plate detector (MarResearch 30 cm diameter). One single cryo-cooled crystal was used for data collection, transferring it to mother liquor containing an addition of 15% PEG 3350, and flash cooled directly into the nitrogen cryo-stream. Diffraction data were autoindexed and integrated using program DENZO, and merged using SCALEPACK (Otwinowski & Minor, 1996) (Table 3). Crystals belong to space group $P2_1$ with unit cell parameters a = 93.4 Å, b = 133.0 Å, c = 122.1 Å, and β = 109.6°. This type of crystal has, as previously reported for native HPII, one tetramer per asymmetric unit and a solvent content of approximately 40% (Bravo et al., 1995).

Refinement, starting with the model of native HPII (Bravo et al., 1998), was carried out using standard protocols in the program XPLOR (Brünger, 1992). The R_{free} criteria were used in all the refinement steps although no reflections were omitted for electron density map calculations. Water molecules were modeled manually using program O (Jones et al., 1990). Bulk solvent correction was also done with XPLOR allowing the use of all reflections in the resolution shell 20.0–2.3 Å. Noncrystallographic symmetry restraints were kept during the refinement to 2.5 Å resolution. Small departures from molecular symmetry appear highly correlated with crystal contacts as also reported for the refined model of wild-type HPII (Bravo et al., 1998). The corresponding final crystallographic agreement factors, R and R_{free}, along with other refinement data, are contained in Table 3.

Solvent accessibilities and cavities were calculated with the program VOIDOO (Kleywegt & Jones, 1994). Atomic radii were chosen in such a way that the sum of the atomic and solvent radii corresponded to observed interatomic distances (Williams et al., 1994). Therefore, van der Waals values were kept for the radii of apolar atoms, while smaller values were used for polar atoms that form hydrogen bonds with water molecules. This modification marginally increases the accessibilities of polar atoms relative to those of apolar atoms. However, it notably improves the visual correlation between solvent accessible volumes and the position of experimentally determined solvent molecules.

Table 3. *Data collection and structural refinement statistics for the Ala260 variant of HPII*

Data collection statistics	
Unique	124,228
$\langle I/\sigma(I)\rangle$	9.0 (2.4)[a]
R_{merge} (%)[b]	7.3 (27.8)
Resolution (Å)	2.3
Completeness (%)	91.5 (93.2)
Structural refinement statistics	
Resolution range (Å)	20–2.3
Number of reflections	($F > 2\sigma$) 112,530
R_{cryst} (%)[c]	19.2
R_{free} (%)[d]	25.3
Number of nonhydrogen atoms	
Protein	22,964
Water	2,751
Heme	176
R_{msd} from ideality	
Bond lengths (Å)	0.022
Bond angles (°)	2.9
Dihedrals (°)	24.4
Improper (°)	1.6
Average B factor (Å^2)	
Main chain	20.6
Side chain	20.7
Water	17.7

[a] Values in parentheses correspond to the highest resolution shell (2.33–2.30 Å).

[b] $R_{merge} = \sum|I - \langle I\rangle|/\sum\langle I\rangle$.

[c] $R_{cryst} = \sum||F_{obs}| - |F_{calc}||/\sum|F_{obs}|$.

[d] R_{free} is as for R_{cryst}, but calculated for a test set comprising reflections not used in the refinement (10%).

Acknowledgments

Work in Barcelona was funded by the DGICYT (PB95-0218) and by the European Union through the HCMP to Large Installations Project (contract CHGE-CT93-0040). Work in Winnipeg was supported by grant OGP9600 from the Natural Sciences and Engineering Research Council of Canada.

References

Berthet S, Nykyri LM, Bravo J, Maté MJ, Berthet-Colominas C, Alzari P, Koller F, Fita I. 1997. Crystallization and preliminary structural analysis of catalase A from *Saccharomyces cerevisiae*. *Protein Sci 6*:481–483.

Bravo J, Fita I, Ferrer JC, Ens W, Hillar A, Switala J, Loewen PC. 1997. Identification of a novel bond between a histidine and the essential tyrosine in catalase HPII on *Escherichia coli*. *Protein Sci 6*:1016–1023.

Bravo J, Maté M, Schneider T, Switala J, Wilson K, Loewen PC, Fita I. 1999. Structure of catalase HPII from *Escherichia coli* at 1.9 Å resolution. *Proteins 34*:155–166.

Bravo J, Verdaguer N, Tormo J, Betzel C, Switala J, Loewen PC, Fita I. 1995. Crystal structure of catalase HPII from *Escherichia coli*. *Structure 3*:491–502.

Brünger AT. 1992. *XPLOR manual version 3*. New Haven, CT: Yale University. 405 pp.

Fita I, Rossmann MG. 1985a. The active center of catalase. *J Mol Biol 185*: 21–37.

Fita I, Rossmann MG. 1985b. The NADPH binding site on beef liver catalase. *Proc Natl Acad Sci USA 82*:1604–1608.

Fita I, Silva AM, Murthy MRN, Rossmann MG. 1986. The refined structure of beef liver catalase at 2.5 Å resolution. *Acta Cryst B 42*:497–515.

Gouet P, Jouve HM, Dideberg O. 1995. Crystal structure of *Proteus mirabilis* PR catalase with and without bound NADPH. *J Mol Biol 249*:933–954.

Hillar A, Nicholls P. 1992. A mechanism for NADPH inhibition of catalase compound II formation. *FEBS Lett 314*:179–182.

Hillar A, Nicholls P, Switala J, Loewen PC. 1994. NADPH binding and control of catalase compound II formation: Comparison of bovine, yeast and *Escherichia coli* enzymes. *Biochem J 300*:531–539.

Kleywegt GJ, Jones TA. 1994. Detection, delineation, measurement, and display of cavities in macromolecules structures. *Acta Cryst D 50*:178–185.

Kunkel TA, Roberts JD, Zakour RA. 1987. Rapid and efficient site specific mutagenesis without phenotypic selection. *Methods Enzymol 154*:367–382.

Jones TA, Zou JY, Cowan SW, Kjeldgaard M. 1990. Improved methods for building protein models in electron density maps. *Acta Cryst 47*:110–119.

Layne E. 1957. Spectrophotometric and turbidimetric methods for measuring proteins. *Methods Enzymol 3*:447–454.

Loewen PC, Switala J. 1986. Purification and characterization of catalase HPII from *Escherichia coli*. K12. *Biochem Cell Biol 64*:638–646.

Loewen PC, Switala J, von Ossowski I, Hillar A, Christie A, Tattrie B, Nicholls P. 1993. Catalase HPII of *Escherichia coli* catalyzes the conversion of protoheme to *cis*-heme *d*. *Biochemistry 32*:10159–10164.

Maté MJ, Zamocky M, NyKyri LM, Herzog C, Alzari PM, Betzel C, Koller F, Fita I. 1999. Structure of catalase A from *Saccharomyces cerevisiae*. *J Mol Biol.* In press.

Mead DA, Skorupa ES, Kemper B. 1985. Single-stranded DNA Sp6 promoter plasmids for engineering mutant RNAs and proteins: Synthesis of a "stretched" preparathyroid hormone. *Nucleic Acids Res 13*:1103–1118.

Mulvey MR, Sorby PA, Triggs-Raine BL, Loewen PC. 1988. Cloning and physical characterization of *katE* and *katF* required for catalase HPII expression in *Escherichia coli*. *Gene 73*:337–345.

Murshudov GN, Grebenko AI, Barynin V, Dauter Z, Wilson KS, Vainshtein BK, Melik-Adamyan W, Bravo J, Ferran JM, Ferrer JC. 1996. Structure of the heme *d* of *Penicillium vitale* and *Escherichia coli* catalases. *J Biol Chem 271*:8863–8868.

Murshudov GN, Melik-Adamyan WR, Grebenko AI, Barynin VV, Vagin AA, Vainshtein BK, Dauter Z, Wilson KS. 1992. Three-dimensional structure of catalase from *Micrococcus lysodeikticus* at 1.5 Å resolution. *FEBS Lett 312*:127–131.

Murthy MRN, Reid TJ, Sicignano A, Tanaka N, Rossmann MG. 1981. Structure of beef liver catalase. *J Mol Biol 152*:465–499.

Ogura Y. 1955. Catalase activity at high concentration of hydrogen peroxide. *Arch Biochem Biophys 57*:288–300.

Otwinowski Z, Minor W. 1996. Processing of X-ray diffraction data collected in oscillation mode. *Methods Enzymol 276*:307–326.

Rørth M, Jensen PK. 1967. Determination of catalase activity by means of the Clark electrode. *Biochim Biophys Acta 139*:171–173.

Sanger FS, Nicklen S, Coulson AR. 1977. DNA sequencing with chain terminating inhibitors. *Proc Natl Acad Sci USA 74*:5463–5467.

Sevinc MS, Switala J, Bravo J, Fita I, Loewen PC. 1998. Truncation and heme pocket mutations reduce production of functional catalase HPII in *Escherichia coli*. *Protein Eng 11:*549–555.

Shimuzu N, Kobayashi K, Hayashi K. 1984. The reaction of superoxide radical with catalase. Mechanism of the inhibition of catalase by superoxide radical. *J Biol Chem 259*:4414–4418.

Takeda A, Miyahara T, Hachimori A, Samejima T. 1980. The interactions of thiol compounds with porcine erythrocyte catalase. *J Biochem 87*:429–439.

Vainshtein BK, Melik-Adamyan WR, Barynin VV, Vagin AA, Grebenko AI. 1981. Three-dimensional structure of the enzyme catalase. *Nature 293*:411–412.

Vainshtein BK, Melik-Adamyan WR, Barynin VV, Vagin AA, Grebenko AI, Borisov VV, Bartels KS, Fita I, Rossmann MG. 1986. Three-dimensional structure of catalase from *Penicillium vitale* at 2.0 Å resolution. *J Mol Biol 188*:49–61.

von Ossowski I, Mulvey MR, Leco PA, Borys A, Loewen PC. 1991. Nucleotide sequence of *Escherichia coli katE*, which encodes catalase HPII. *J Bacteriol 173*:514–520.

Williams MA, Goodfellow JM, Thornton JM. 1994. Buried waters and internal cavities in monomeric proteins. *Protein Sci 3*:1224–1235.

Yanisch-Perron C, Vietra J, Messing J. 1985. Improved M13 phage cloning vectors and host strains: Nucleotide sequence of the M13mp18 and pUC19 vectors. *Gene 33*:103–119.

Zamocky M, Herzog C, NyKyri LM, Koller F. 1995. Site-directed mutagenesis of the lower parts of the major substrate channel of yeast catalase A leads to highly increased peroxidatic activity. *FEBS Lett 367*:241–245.